

Supplement Material

for

A significant mechanism of stratospheric O₃ intrusion to atmospheric environment: a case study of North China Plain

Yuehan Luo¹, Tianliang Zhao^{1,*}, Kai Meng², Jun Hu³, Qingjian Yang¹, Yongqing Bai⁴, Kai Yang¹, Weikang Fu¹, Chenghao Tan^{5,6}, Yifan Zhang⁷, Yanzhe Zhang⁸, Zhikuan Li¹

¹Collaborative Innovation Center on Forecast and Evaluation of Meteorological Disasters, Key Laboratory of Aerosol-Cloud-Precipitation of China Meteorological Administration, Nanjing University of Information Science and Technology, Nanjing, 210044, China

²Key Laboratory of Meteorology and Ecological Environment of Hebei Province, Hebei Provincial Institute of Meteorological Sciences, Shijiahuang, 050021, China

³Fujian Academy of Environmental Sciences, Fuzhou, 350011, China

⁴Hubei Key Laboratory for Heavy Rain Monitoring and Warning Research, Institute of Heavy Rain, China Meteorological Administration, Wuhan, 430205, China

⁵State Key Laboratory of Organic Geochemistry, Guangzhou Institute of Geochemistry, Chinese Academy of Sciences, Guangzhou 510640, Guangdong, China

⁶University of Chinese Academy of Sciences, Beijing 100049, China

⁷Xuchang Meteorological Service, Xuchang, 450003, China

⁸Ningxia Air Traffic Management Sub-bureau of CAAC, Yinchuan, 750009, China

Correspondence to: Tianliang Zhao (tlzhao@nuist.edu.cn)

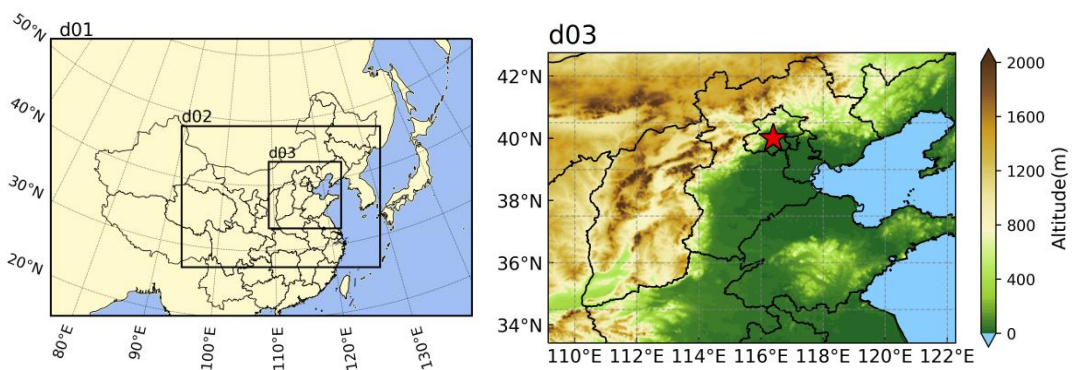


Figure S1: The spatial distributions of three nesting domains d01, d02 and d03 with terrain altitude (m in a.s.l.). The red star represents the capital of China, Beijing.

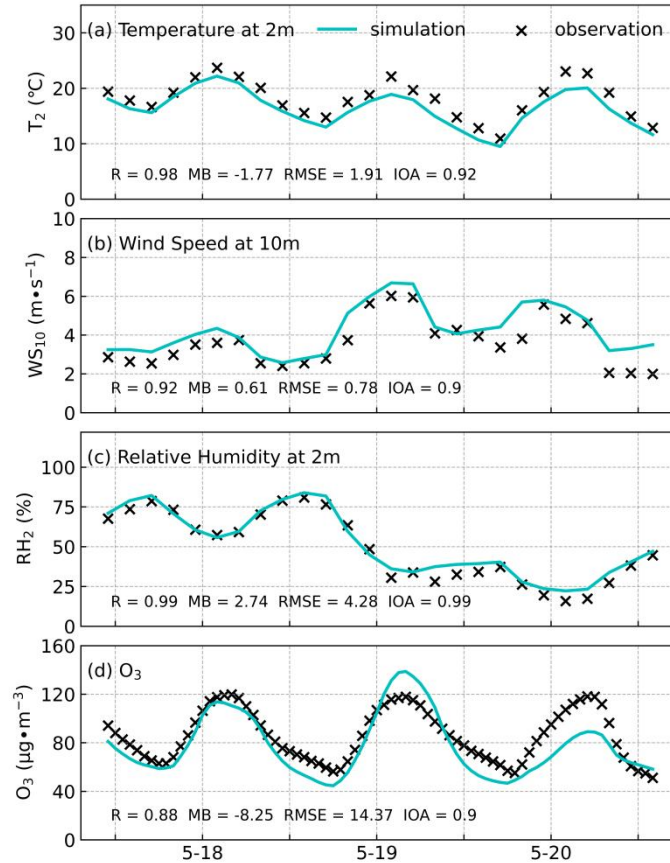


Figure S2: Hourly changes of simulated and observed meteorological elements and near-surface O_3 concentrations during May 18–20, 2019 averaged over North China.

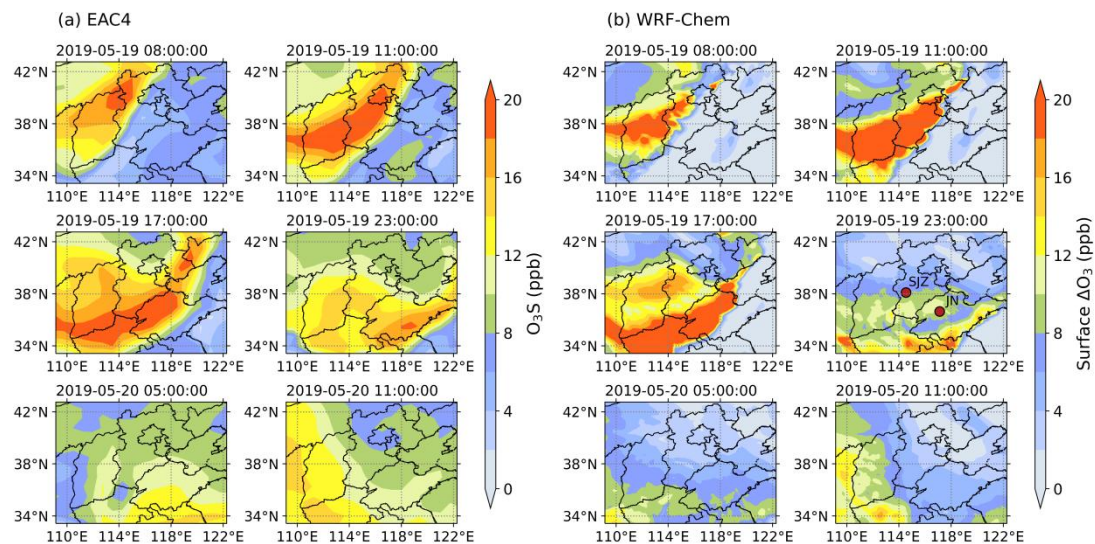


Figure S3: Spatial distribution of (a) the surface O_3S derived from EAC4 data and (b) the differences of surface O_3 between $\text{CASE}_{\text{STRO}_3}$ and $\text{CASE}_{\text{noSTRO}_3}$ simulations of WRF-Chem over the NCP. The red dots in (b) indicate the geographical location of the representative sites SJZ and JN in the NCP.

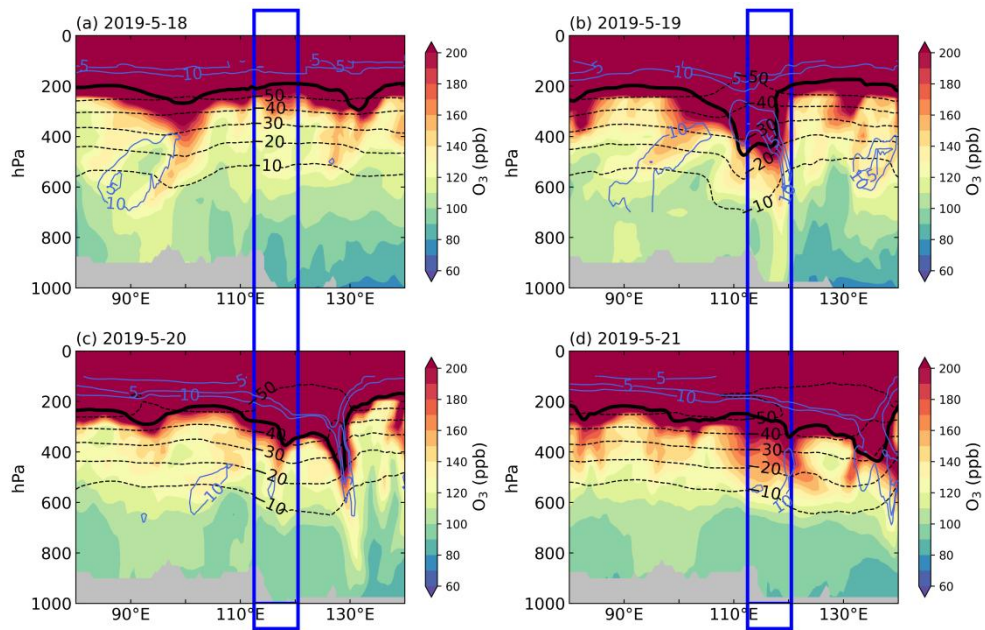


Figure S4: Latitudinal vertical sections of O₃ concentrations (color contours) averaged over 32 °N–40 °N from the MERRA2 data during May 18–21, 2019. Black solid lines indicate the dynamical tropopause labeled by PV=2. The dashed black lines represent air temperature (°C), the solid blue lines represent relative humidity (%), and the blue rectangles mark the NCP region.

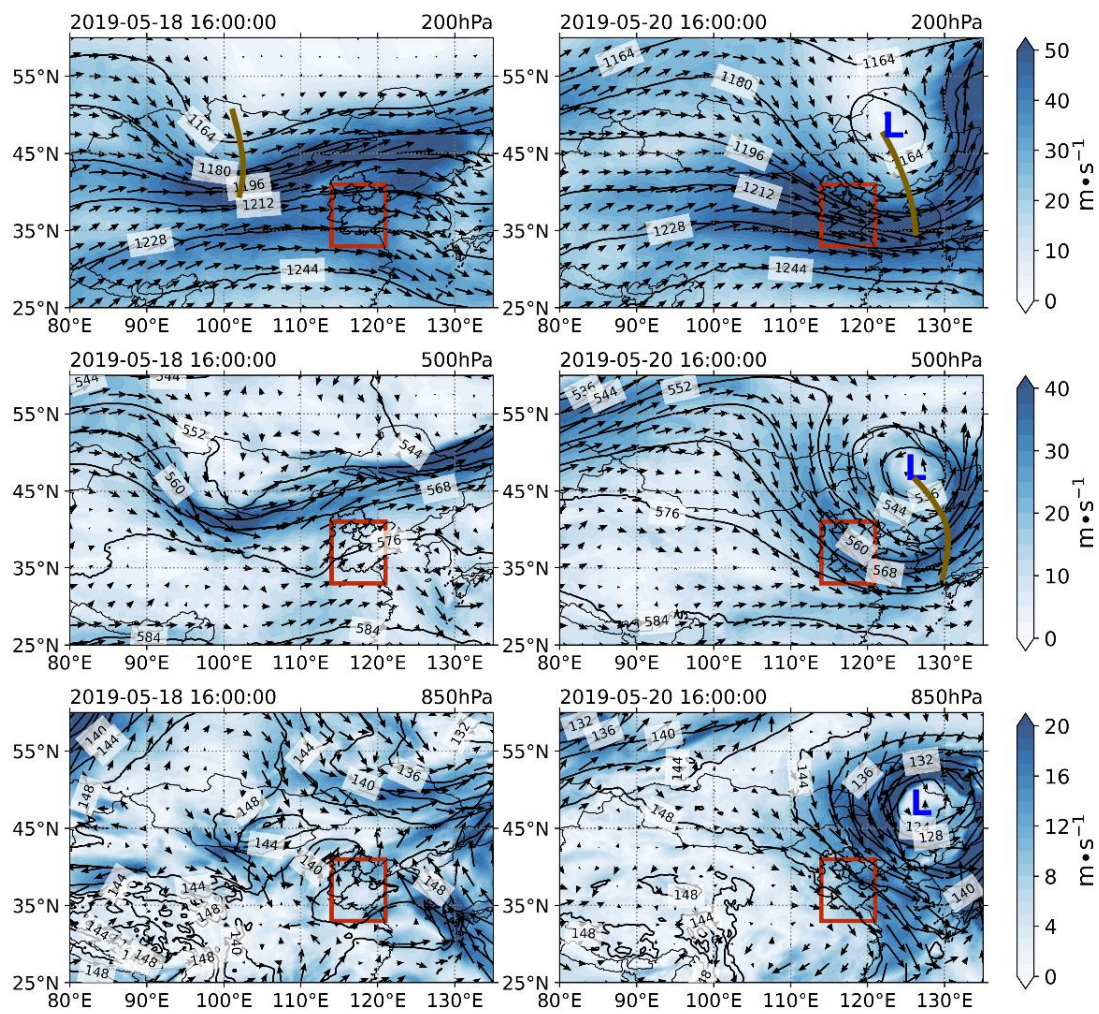


Figure S5: Atmospheric circulation patterns of horizontal wind vectors at 200 hPa, 500 hPa, and 850 hPa at 16:00 LST on May 18 and 20, 2019. The shaded colors and black arrows denote the horizontal wind speed ($\text{m}\cdot\text{s}^{-1}$), and the black contour lines denote the geopotential height (gpm). The red solid boxes indicate the scope of the NCP region.

Table S1: Physical and chemical parameterization schemes used in the WRF-Chem simulations.

Process	Parameters	WRF-Chem options
Physical process	Microphysics	Lin scheme
	Longwave radiation	RRTM scheme
	Shortwave radiation	Goddard scheme
	Boundary layer	YSU scheme
	Land surface	unified Noah land-surface model
	Surface layer	MM5 similarity scheme
	Cumulus	Grell 3D ensemble scheme
Chemical process	Gas-phase chemistry	CBMZ
	Aerosol module	MOSAIC_8bins